

Band-structure calculations of the half-metallic ferromagnetism and structural stability of full- and half-Heusler phases

T. Block, M. J. Carey, and B. A. Gurney

Hitachi San Jose Research Center, 650 Harry Road, San Jose, California 95120, USA

O. Jepsen

Max-Planck-Institut für Festkörperforschung, Heisenbergstr. 1, 70569 Stuttgart, Germany

(Received 11 August 2004; published 12 November 2004)

Self-consistent first principle calculations within the local density approximation were used to study the effect of lattice distortions on the electronic and magnetic properties of half (NiMnSb) and full-Heusler (Co_2CrAl) compounds. We find that NiMnSb is half-metallic from -2% to $+3\%$ uniform strain, whereas Co_2CrAl is half-metallic from -1% to $+3\%$. The loss of the half-metallic character is primarily due to a shift in the density of states relative to the Fermi energy. Under tetragonal distortions, high spin polarization at the Fermi level is maintained over a larger range, but the gap width is strongly affected. Therefore, only nonuniform strain should not be the expected reason for the poor performance of Heusler compounds in spintronic devices. The impacts of these results on spintronic devices are discussed.

DOI: 10.1103/PhysRevB.70.205114

PACS number(s): 71.20.Be, 71.20.Lp

Since de Groot *et al.*¹ predicted NiMnSb to be the first half-metallic ferromagnet, Heusler compounds have received much study due to their potential as key materials for spintronic devices.^{2,3} Further Heusler compounds like Mn_2VAl ,⁴ Co_2MnX ($X=\text{Si, Ge, Sn}$),⁵ Co_2MnZ ($Z=sp$ elements),⁶ Ru_2MnZ ($Z=\text{Si, Ge, Sn and Sb}$),⁷ Co_2MnZ ($Z=\text{Si, Ge}$)⁸ attracted also much attention. At the Fermi energy (E_F) one spin direction is metallic and the other has an energy gap, resulting in 100% spin polarization (P). Thus they can be used for perfect spin filters,⁹ spin-injection devices¹⁰ or magnetoresistive devices with infinite magnetoresistance (MR). Research groups investigated different physical properties of the Heusler alloys. Magneto-optical properties¹¹ and noncollinear spin ordering¹² of the Heusler alloys were studied. Lately the interest has been focused on the origin of the half-metallic gap^{13–15} and spin-orbit interaction¹⁶ in these compounds. Non-Heusler half-metallic ferromagnets exist,^{17–20} but the Heusler compounds are desirable for applications due to their high Curie temperatures and low coercivities. Some results assume that a symmetry break of the high ordered surfaces takes place and 100% spin polarization occurs under careful conditions at NiMnSb/CdS-interfaces.²¹ The interface geometry and their influence on the electronic and magnetic properties has been investigated also for $\text{Co}_2\text{MnGe}/\text{GaAs}$ interfaces.²²

Unfortunately, other direct observations^{23–25} have only found P values up to 58%. High MR has not been observed in spin valves using Heusler layers,²⁶ but has been observed in powder compacts,²⁷ suggesting that high P in thin films is particularly difficult to obtain. Thin films are far from the perfect, infinite crystals used for band structure calculations. Impurities like the small Pt doping influence P the electronic and magnetic properties of the Heusler compounds.²⁸ Moreover, are the surface and interface properties of half-metallic materials potentially of crucial importance to their proposed spin-electronic device applications.^{29,30} Band structure calculations suggest that atomic site disorder³¹ and structural

defects³² reduce the half-metallic character. Miura *et al.* confirmed these results in a recent publication for the full-Heusler alloys $\text{Co}_2(\text{Cr}_{1-x}\text{Fe}_x)\text{Al}$.³³ However, the impact of structural deviations from the perfect crystal structure on P has not been studied sufficiently.

In this paper we present the results of self-consistent first principle calculations which show the effect of uniform strain and tetragonal distortion on the electronic and magnetic properties of selected Heusler compounds. We compare results from half-Heusler (NiMnSb) and full-Heusler (Co_2CrAl) compounds. In particular, we find that deviations of a few percent from the bulk lattice parameter result in a loss of 100% P . These result from two mechanisms: a shift of E_F away from the gap and a closing of the gap width, E_{gap} . Both effects are observed for both uniform strain and tetragonal distortion. However, we find that the loss in P can be primarily attributed to the shift in E_F for the uniform strain case and the closing of E_{gap} for the tetragonal distortion case. In addition, our band structure calculations with the linear augmented plane wave method³⁴ confirmed our presented results for the same study.³⁵

In the present work, we used the tight-binding linear muffin-tin orbital in the atomic sphere approximation.³⁶ We used the exchange-correlation potential suggested by von Barth and Hedin³⁷ with the assumption of a magnetic ground state (spin-polarized calculation), as these yielded more stable total energies due to the magnetic ordering. The k integrated functions were evaluated by the tetrahedron method³⁸ in a grid of at least 1800 k points in the irreducible part of the Brillouin zone.³⁹ The positions and radii of the interstitial spheres were calculated using an automated procedure developed by Krier *et al.*⁴⁰ The scalar relativistic Kohn-Sham-Schrödinger equations were solved taking all relativistic effects into account except for the spin-orbit coupling. Calculations were performed for infinite crystals to isolate the effects of strain and distortion. The effects of thin layers and interfaces are planned for a future publication.

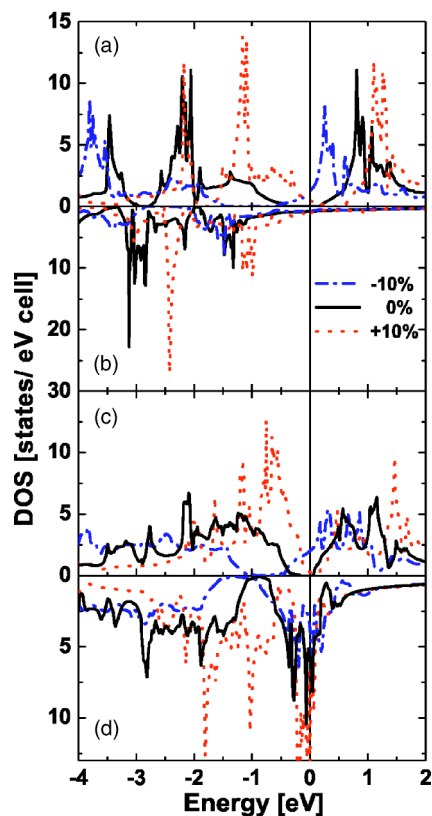


FIG. 1. DOS for half- and full-Heusler compounds under uniform strain. Shown are NiMnSb (a) minority and (b) majority and Co₂CrAl (c) minority and (d) majority spins. Data are shown for +10%, -10% and the unstrained case.

We calculated the electronic structure by using a supercell structure with 4 formula units (f.u.) in the cell. Starting point for the calculations were the compounds with 0 percent strain and lattice parameters of $a=5.903$ Å for NiMnSb, 5.727 Å for Co₂CrAl, respectively.⁴¹ Calculations were performed for uniform strains from -10% to +10% relative to the experimental lattice parameter 5.313 – 6.493 Å for NiMnSb and 5.154 Å– 6.300 Å for Co₂CrAl. A nonuniform strain is more likely in a layered system where epitaxial strains from adjacent layers can be significant. Thus, we also studied the effect of a tetragonal distortion with the c axis varied from -15% to +15% relative to the equilibrium with the volume of the unit cell constant ($a=6.414$ – 5.514 Å, $c=5.452$ – 6.341 Å for NiMnSb). Co₂CrAl changes the lattice parameters for a from 6.212 to 5.340 Å and c from 5.280 to 6.142 Å. While the extremes of these strains are quite large, they were chosen for three reasons. First, the shape memory Heusler alloys have shown the capacity for tetragonal distortions of 9%.⁴² Second, the lattice mismatches expected in a spin valve are also rather large. Copper is often used in spin valves applications due its long spin-diffusion length, but the mismatch between Cu ($a=3.61$ Å) and Co₂CrAl is 37%.⁴³ Last, the range of distortions was chosen to clearly show the trends in the density of states (DOS) results.

A detailed description of the unstrained NiMnSb band structure is given in Ref. 1, but some important features from our calculations must be mentioned to describe the influence

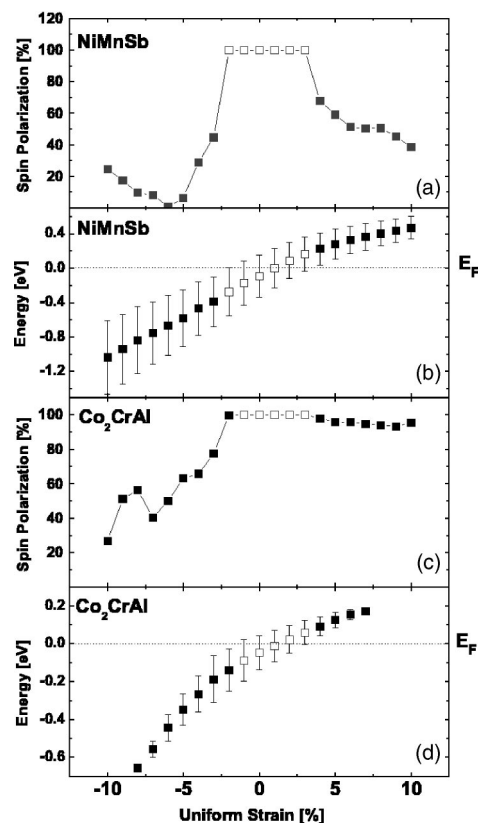


FIG. 2. Effect of uniform strain on spin polarization and gap for NiMnSb (a) and (b) and Co₂CrAl (c) and (d). The gap center is shown via points and E_{gap} is shown via error bars. Data points are hollow for the cases with 100% spin polarization. The spin polarizations, (a) and (c), are 100% near zero strain. The Fermi energy is shown by the horizontal lines in (b) and (d).

of the uniform strain and distortion. NiMnSb is a half-metal with a total spin moment of $4\mu_B$ /f.u. due to the strong exchange splitting of the Mn $3d$ ($3.73\mu_B$) electrons. Compared to this, the Ni $3d$ electrons are weakly spin-polarized ($0.29\mu_B$). Sb has a spin moment of $-0.06\mu_B$. The Ni-Mn interactions, as the strongest bonding interactions, determine the formation of the gap of 0.25 eV.

Our calculations show that Co₂CrAl has local magnetic moments of $0.77\mu_B$ on Co and $1.54\mu_B$ on Cr. The interaction between the transition metals is ferromagnetic, leading to a total calculated moment of $3.0\mu_B$. The calculated total DOS (TDOS) shows a gap of 0.18 eV for minority spin electrons. The gap in the minority bands is due to the Co-Cr interactions as the strongest bonding interactions. This covalent hybridization is the reason for the formation of bonding and antibonding states and determines the position of E_F .²⁷ Cr states are completely polarized, with an exchange splitting of 1.1 eV. The splitting between the Co majority and minority bands is smaller (0.8 eV). The Al states are only slightly polarized, due to a weak bonding between Cr and Al.

The spin-projected TDOS of the uniformly strained compounds are shown in Figs. 1(a) and 1(b) (NiMnSb) and 1(c) and 1(d) (Co₂CrAl). Hereafter the DOS presented on the upper half plane of each figure corresponds to the minority and the lower to the majority channel. The vertical lines

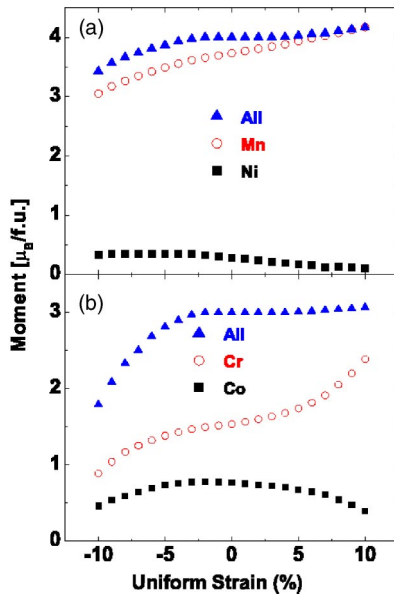


FIG. 3. Total magnetic moment and partial magnetic moment of Ni and Mn in NiMnSb (a) and Co and Cr in Co₂CrAl (b) in units of μ_B per f.u. as function of axial strain.

indicate the position of E_F ($E_F=0$). The centers of the gaps shift relative to E_F . E_{gap} changes slightly with strain, however, the lattice strain does not change the general shapes of the TDOSs of NiMnSb and Co₂CrAl. The trends for P , the center position and width of the gap are shown in Fig. 2. We calculated the spin polarization as the ratio $(n_{\uparrow}-n_{\downarrow})/(n_{\uparrow}+n_{\downarrow})$, where n_{\uparrow} and n_{\downarrow} are the majority and minority DOS at E_F , respectively. P is shown in Figs. 2(a) (NiMnSb) and 2(c) (Co₂CrAl). We observe that 100% P is only observed from -2% to $+3\%$ for NiMnSb and from -1% to $+3\%$ for Co₂CrAl. P drops rapidly for negative strains in both compounds and for NiMnSb with positive strain. The polarization remains $>90\%$ up to $+10\%$ strain for Co₂CrAl. The gap center is plotted relative to the Fermi energy ($E_F=0$) in Figs. 2(b) (NiMnSb) and 2(d) (Co₂CrAl). The gap center is shown via points, and E_{gap} is shown via error bars. The gap center has a positive slope, as expected.⁴⁴ E_{gap} in the minority channel decrease monotonically for strains between -10% to $+10\%$ from 0.42 to 0.13 eV for NiMnSb. The trend for Co₂CrAl is not monotonic. E_{gap} has a maximum of 0.25 eV at -3% and is missing at the extremes. The slope is much steeper for NiMnSb.

The principal reason for the loss of the half-metallic character is due to the shift of the bands relative to E_F . Negative strain corresponds to a squeeze of the lattice. The resulting smaller volume of the unit cell causes broader bands. Due to steeper bands the dispersion of the electronic states is larger. A charge transfer from the majority so the minority spins takes place. Positive strain has the opposite effect. The changes of the center and the width of the gap from negative to positive strain can be described as follows: The electrons become more localized and the exchange coupling increases. Due to that the minority bands are shifted higher relative to the majority bands, with the consequent increased depopulation of the minority bands. Figure 3 shows how the magnetic

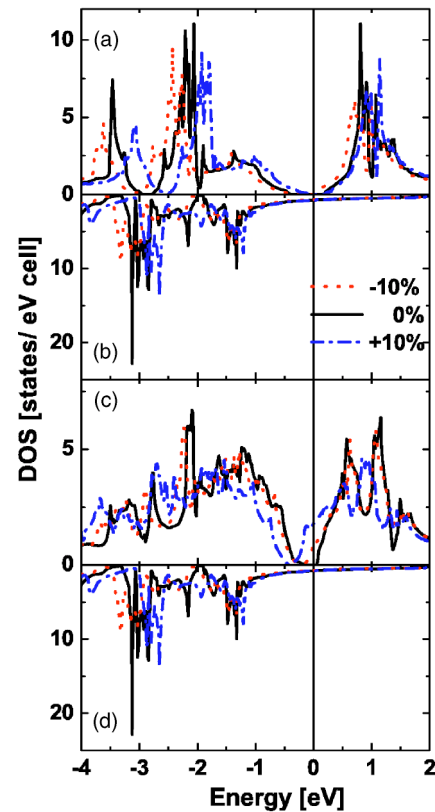


FIG. 4. DOS for half- and full-Heusler compounds under tetragonal distortion. Shown are NiMnSb (a) minority and (b) majority and Co₂CrAl (c) minority and (d) majority spins. Data are shown for $+10\%$, -10% and the unstrained case.

moments vary with strain. An integral total moment is a necessary condition for 100% P . The total magnetic moment of NiMnSb is exactly $4\mu_B$ [Fig. 3(a)]; μ_{Ni} decreases and μ_{Mn} increases as the lattice is expanded. As long as the changes of the magnetic moments compensate each other, the half-metal behavior is retained. The widening of the lattice is associated with a weaker bonding between the transition metals. The noticeable strong covalent bonding interactions between the transition metals is a particular property of the Heusler phases. When the covalent hybridization between the transition metals decreases it is combined with a loss of the half-metallic character.⁴⁵ The band character of Mn is more isolated and the moments converge to the values of the single atom, i.e., to $5\mu_B$. The compression has the opposite effect up to -7% strain. At less than -7% the partial magnetic moments on Ni also decrease. The behavior of the partial magnetic moments in Co₂CrAl is similar for an expansion of the lattice and is similar to NiMnSb. Therefore, the change of the partial magnetic moment for a compression of the lattice is different. It lowers μ_{Co} for $<-2\%$ strain, concurrently, μ_{Cr} is also decreasing, but earlier compared to NiMnSb. As a consequence, a rapid lowering of the total magnetic moment appears for $<-3\%$ strain.

The TDOS is shown in Fig. 4 for tetragonal distortion. The shifts in E_F are very small compared to the uniform strain case. Figure 5 displays the influence of tetragonal distortion on P and E_{gap} . NiMnSb is not very sensitive to te-

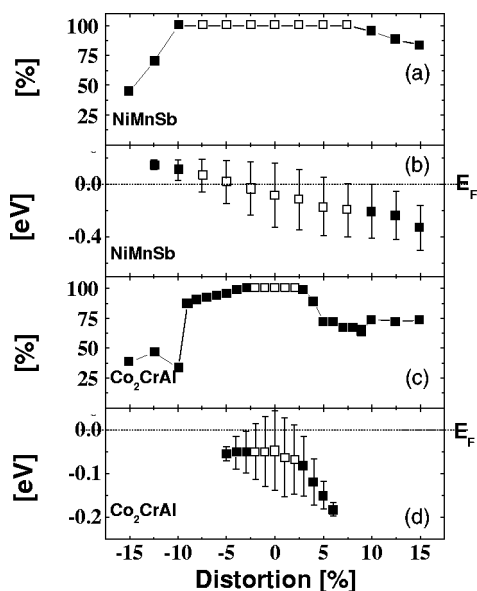


FIG. 5. Effect of tetragonal on spin polarization and gap for NiMnSb (a) and (b) and Co₂CrAl (c) and (d). Data points are hollow for the cases with 100% spin polarization. The Fermi energy is shown by the horizontal lines in (b) and (d). Note the different scale for the energies in (b) and (d). The gap does not move relative to E_F as much as in the uniform strain case.

tetragonal distortion with retention of the half-metallic character in the range from -7.5% to 7.5% . This fact is surprising due to the resulting lowering of the symmetry and compared to the behavior of NiMnSb on uniform strain. Co₂CrAl is more sensitive to tetragonal distortion, with $P=100\%$ only for the range -2% to 2% [Fig. 5(c)]. The higher sensitivity is due in part to the smaller E_{gap} for Co₂CrAl. The trend of E_{gap} with distortion is not monotonically decreasing as with NiMnSb. In addition, pseudogaps appear when the lattice is compressed more than -6% and expanded over $+6\%$. The formation of pseudogaps is also known from the full-Heusler phase Fe₂VAl (Ref. 46) and destroys the half-metallic character.

The trends in the local magnetic moments underline the earlier behavior. For both NiMnSb [Fig. 6(a)] and Co₂CrAl [Fig. 6(b)] the moments of the constituent atoms vary much less than in the uniform strain case. For NiMnSb, the slopes of the μ_{Ni} and μ_{Mn} follow opposite trends as in the uniform strain case. μ_{Ni} and μ_{Mn} complement each other leading to a $4.0 \mu_B$ total moment over a large range. For Co₂CrAl, μ_{Co} and μ_{Cr} compensate each other well over the range from -10% to $+2.5\%$. They diverge above 2.5% leading to the drop in P observed in Fig. 5(c). Negative tetragonal distortion decreases the hybridization between Co and Cr. Cr con-

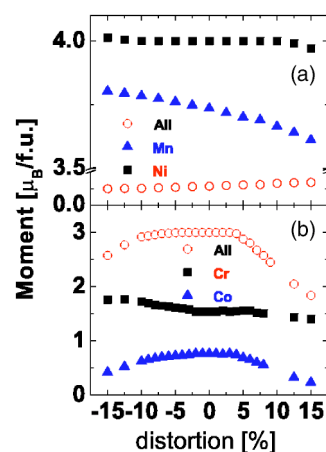


FIG. 6. Total magnetic moment and partial magnetic moment of Ni and Mn in NiMnSb (a) and Co and Cr in Co₂CrAl (b) in units of μ_B per f.u. as function of axial strain.

verges to the spin moment of the atomic value. The positive distortion causes a decrease of both spin moments. The hybridization between Co and Cr is weaker than in the undistorted structure. The remarkable fact is due to a simultaneous decrease of the spin moments. E_F is shifting in the same direction to higher energies for tetragonal expansion or compression.

The loss of 100% P due to stain and distortion has a direct impact on the application of Heusler compounds to devices. Sputtered films can have stresses of $\pm 1\text{GPa}$ due to the deposition process alone.⁴⁷ Thus, careful control of deposition conditions will be required for optimal results. As noted earlier, the epitaxial mismatches with Cu are very large. The same will be true for most elemental or simple alloy layers, so some ordered alloy is likely required. Thus, we need to find a spacer layer which can meet three criteria: (1) a long spin diffusion length, (2) a good lattice match, and (3) a good band match with the Heusler compound.

In conclusion, the self-consistent band structure calculations indicate that the half-metallic character of the Heusler phases is lost with only a few percent uniform stress or tetragonal distortion of the lattice. We find that for uniform strain the loss is primarily due to a shift of E_F away from the gap. For tetragonal distortion the loss results from a closing of the gap. We explained this behavior with the varying changes of the hybridization between the transition elements which is the important feature for the formation of the half-metallic gap.

The authors thank F. Rocker for help with installation of the LMTO code.

¹R. A. de Groot, F. M. Mueller, P. G. van Engen, and K. H. J. Buschow, Phys. Rev. Lett. **50**, 2024 (1983).

²S. A. Wolf, D. D. Awschalom, R. A. Buhrman, J. M. Daughton, S. von Molnar, M. L. Roukes, A. Y. Chtchelkanova, and D. M. Treger, Science **294**, 1488 (2001).

³C. M. Fang, G. A. de Wijs, and R. A. de Groot, J. Appl. Phys. **91**, 8340 (2002).

⁴R. Weht and W. E. Pickett, Phys. Rev. B **60**, 13 006 (1999).

⁵S. Picozzi, A. Continenza, and A. J. Freeman, Phys. Rev. B **66**, 094421 (2002).

- ⁶S. Ishida, S. Fujii, S. Kashiwagi, and S. Asano, *J. Phys. Soc. Jpn.* **64**, 2152 (1995).
- ⁷S. Ishida, S. Kashiwagi, S. Fujii, and S. Asano, *Physica B* **210**, 140 (1995).
- ⁸S. Ishida, T. Masaki, S. Fujii, and S. Asano, *Physica B* **245**, 1 (1998).
- ⁹K. A. Kilian and R. H. Victora, *J. Appl. Phys.* **87**, 7064 (2000).
- ¹⁰S. Datta and B. Das, *Appl. Phys. Lett.* **56**, 665 (1990).
- ¹¹R. A. de Groot, F. M. Mueller, P. G. van Engen, and K. H. J. Buschow, *J. Appl. Phys.* **55**, 2151 (1984).
- ¹²P. Mohn and E. Supanetz, *Philos. Mag. B* **78**, 629 (1998).
- ¹³I. Galanakis, P. H. Dederichs, and N. Papanikolaou, *Phys. Rev. B* **66**, 134428 (2002).
- ¹⁴I. Galanakis, P. H. Dederichs, and N. Papanikolaou, *Phys. Rev. B* **66**, 174429 (2002).
- ¹⁵I. Galanakis, *J. Phys.: Condens. Matter* **14**, 6329 (2002).
- ¹⁶P. Mavropoulos, K. Sato, R. Zeller, P. H. Dederichs, V. Popescu, and H. Ebert, *Phys. Rev. B* **69**, 054424 (2004).
- ¹⁷A. Gupta and J. Z. Sun, *J. Magn. Magn. Mater.* **200**, 24 (1999).
- ¹⁸H. Y. Hwang and S.-W. Cheong, *Science* **278**, 1607 (1997).
- ¹⁹R. von Helmold, J. Wecker, B. Holzapfel, L. Schultz, and K. Samwer, *Phys. Rev. Lett.* **71**, 2331 (1993).
- ²⁰W.-H. Xie, Y.-Q. Xu, B.-G. Liu, and D. G. Pettifor, *Phys. Rev. Lett.* **91**, 037204 (2003).
- ²¹G. A. de Wijs and R. A. de Groot, *Phys. Rev. B* **64**, 020402 (2001).
- ²²S. Picozzi, A. Continenza, and A. J. Freeman, *J. Phys. Chem. Solids* **64**, 1697 (2003).
- ²³W. Zhu, B. Sinkovic, E. Vescovo, C. Tanaka, and J. S. Moodera, *Phys. Rev. B* **64**, 060403 (2001).
- ²⁴K. Inomata, S. Okamura, R. Goto, and N. Tezuka, *Jpn. J. Appl. Phys., Part 2* **42**, L419 (2003).
- ²⁵R. J. Soulen, J. M. Byers, M. S. Osofsky, B. Nadgorny, T. Ambrose, S. F. Cheng, P. R. Broussard, C. T. Tanaka, J. Nowak, J. S. Moodera, A. Barry, and J. M. D. Coey, *Science* **282**, 85 (1998).
- ²⁶J. A. Caballero, A. C. Reilly, Y. Hao, J. Bass, W. P. Pratt, F. Petroff, and J. R. Childress, *J. Magn. Magn. Mater.* **199**, 55 (1999).
- ²⁷T. Block, C. Felser, G. Jakob, J. Ensling, B. Mühling, P. Gütlich, and R. J. Cava, *J. Solid State Chem.* **176**, 646 (2003).
- ²⁸M. Pugaczowa-Michalska, *Acta Phys. Pol. A* **103**, 393 (2003).
- ²⁹S. J. Jenkins and D. A. King, *Surf. Sci.* **501**, L185 (2002).
- ³⁰S. J. Jenkins and D. A. King, *Surf. Sci.* **494**, L793 (2001).
- ³¹D. Orgassa, H. Fujiwara, T. C. Schulthess, and W. H. Butler, *Phys. Rev. B* **60**, 13 237 (1999).
- ³²S. Picozzi, A. Continenza, and A. J. Freeman, *Phys. Rev. B* **69**, 094423 (2004).
- ³³Y. Miura, K. Nagao, and M. Shirai, *Phys. Rev. B* **69**, 144413 (2004).
- ³⁴P. Blaha, K. Schwarz, G. K. H. Madsen, D. Kvasnicka, and J. Luitz, *WIEN2k, An Augmented Plane Wave + Local Orbitals Program for Calculating Crystal Properties* (Karlheinz Schwarz, Techn. Universität Wien, Austria, 2001).
- ³⁵T. Block and M. J. Carey (unpublished).
- ³⁶O. K. Andersen and O. Jepsen, *Phys. Rev. Lett.* **53**, 2571 (1984).
- ³⁷U. von Barth and L. Hedin, *J. Phys. C* **5**, 1629 (1972).
- ³⁸P. E. Blöchl, O. Jepsen, and O. K. Andersen, *Phys. Rev. B* **49**, 16 223 (1994).
- ³⁹C. J. Bradley and A. P. Cracknell, *The Mathematical Theory of Symmetry in Solids* (Clarendon, Oxford, 1972).
- ⁴⁰G. Krier, O. Jepsen, and O. Andersen (unpublished).
- ⁴¹K. H. J. Buschow, P. G. van Engen, and R. Jongebreur, *J. Magn. Magn. Mater.* **38**, 1 (1983).
- ⁴²A. Sozinov, A. A. Likhachev, N. Lanska, and K. Ullakko, *Appl. Phys. Lett.* **80**, 1746 (2002).
- ⁴³The mismatch between Cu and the Cr sublattice of Co₂CrAl is 11%. This requires Cu[100]/Co₂CrAl[110].
- ⁴⁴ $E_F \propto V^{-2/3}$ for a free electron gas.
- ⁴⁵T. Block, Ph.D. thesis, Johannes Gutenberg-Universität Mainz, Germany, 2002.
- ⁴⁶D. J. Singh and I. I. Mazin, *Phys. Rev. B* **57**, 14 352 (1998).
- ⁴⁷T. J. Vink, M. A. J. Somers, J. L. C. Daams, and A. G. Dirks, *J. Appl. Phys.* **70**, 4301 (1991).